

3
4 **Effects of Residual Cirrus and Temperature Biases on Ozone Distributions from the V6**
5 **Level 3 Dataset**

6 Residual cirrus contamination effects are present in both the V6 Level 2 profiles and in the Level
7 3 (map coefficient) product used for this study. As an example, Figure S1 is a map of the
8 distribution of V6 ozone at the 68-hPa level on 15 March 1979, as those effects appear as
9 sporadic excesses of tropical ozone. Those excesses appear to extend over large longitude
10 intervals because there are wave coefficients for only one to two zonal waves. V6 nitric acid has
11 weaker excesses at 68 hPa at the same locations as shown in Figure S2. The LIMS nitric acid
12 channel is centered in the atmospheric window region near 11 μm , and its forward model is
13 optically thin compared to that for ozone. Thus, the nitric acid profiles serve as separate
14 although less sensitive indicators of the presence of residual cirrus.

15
16 Temperature biases are evaluated for a test day, 26 January 1979. Figure S3 shows the bias
17 profile for the latitude range of 40°S to 20°S. It is of order -0.7 K from 30 to 50 hPa compared
18 to MERRA data (c.f., Fig. 2 for 20°S to 20°N of the parent manuscript). Retrieved V6 ozone is
19 very sensitive to temperature bias in the lower stratosphere, such that a -0.7 K bias leads to an
20 ozone error of order +15%. The V6 temperatures also have larger negative values below the
21 100-hPa level, and its associated retrieved V6 ozone is not accurate. On the other hand, mean
22 temperature biases from 20°N to 40°N (not shown) are only of order -0.2 K from 30 to 50 hPa.

23
24 Figure S4 is for ozone from 40°S to 20°S, and the mean differences (bottom left) are negative at
25 10 hPa, tending to zero at about 50 hPa. The temperature bias of Fig. S3 changes to +1.4 K at
26 100 hPa and leads to zero values of retrieved V6 ozone in Fig. S4. Standard deviations about the
27 zonal mean are small at 50 hPa and of the order 0.2 ppmv for MERRA and 0.3 ppmv for V6
28 ozone (Fig. S4--top right). It is noted also that MERRA ozone perturbations from a SBUV
29 control run are constrained somewhat in the tropics, but less so at middle latitudes.

30
31 What are the distributions of SCO and TRCO on 26 January? First, Figure S5 is the plot of
32 TOMS ozone for that day, where the broad, white swath near 50°E is the region where TOMS
33 made no measurements that day. Figure S6 is the distribution of V6 SCO, and it shows relatively
34 large values of 240 DU in the latitude band of 40 to 50°S and minimum values of order 210 DU
35 in the tropics. Figure S7 is the associated distribution of TRCO values, where the red dot is the
36 location of Santiago, Chile, or along the elevated Andes range of South America. The latitude
37 zone of 30 to 50°S has large variations of -60 to 120 DU. A part of the largest positive TRCO
38 values may be where the tropopause was below the 100-hPa level and where a fraction of those

39 TRCO values may be between 100 hPa and the tropopause or in the lowermost stratosphere. The
40 negative values occur at longitudes where ozone at higher southern latitudes is normally low (see
41 February average in Ziemke et al. 2006), and where there may have been transport of low ozone
42 to lower latitudes in late January. Figure S8 shows zonal eddy geopotential height contours at
43 100 hPa on 26 January. The circulation near 50°S, 30°W longitude appears to be moving low
44 ozone from high to middle southern latitudes on 26 January.

45

46 There are significant zonal wave variations in temperature of order 4 to 5 K in the lowermost
47 stratosphere at SH middle latitudes (see Fig. S3 at upper right), and the V6 temperatures in some
48 narrow latitude zones may have biases that vary from positive to even more negative than -0.7 K
49 between 40°S and 20°S. The V6 Level 3 zonal wave temperature coefficients have a relatively
50 poor fit to the Level 2 profile data (rms deviations of 2.5 to 4 K at 36°S) at the levels of 21 to
51 100 hPa. In other words, the Level 3 algorithm smooths the amplitudes of the zonal wave
52 coefficients (see next paragraphs). Figure S9 is a plot of the V6 temperature distribution at 46
53 hPa, showing that there are strong meridional temperature gradients at about 35°S and at 25°N.
54 Fig. S9 also shows zonal wave-4 to wave-5 features at the SH middle latitudes, characteristic of
55 baroclinic, medium wave forcing effects from below during summer.

56

57 A small part of the zonal ozone variations at middle latitudes ($\pm 20^\circ$ to 40°) is because of the
58 along site temperature gradient corrections. That prospect is illustrated more clearly with Figure
59 S10, which is the zonal mean, latitude versus pressure plot of V6 temperatures for 26 January.
60 Note that there are strong meridional gradients at about 30°S and 25°N and from about 50 to 100
61 hPa. Those two latitudes are where corrections for horizontal temperature gradients are
62 important for accurate retrievals of both temperature and ozone (Remsberg et al., 2007).
63 Estimates of temperature gradients for the processing of the V6 profiles were obtained from
64 analyses on pressure surfaces of the V5 temperature fields. However, the V5 profile retrievals
65 were carried out only at every 4° of latitude along orbits, such that its meridional gradients are
66 limited by that coarse latitude spacing. In other words, the V5 temperature fields underestimate
67 the actual meridional gradients for retrievals of V6 temperature and ozone profiles, which were
68 processed at every 1.6° of latitude. Figure S11 is a further example, showing a zonal mean cross
69 section of the V6 minus V5 temperatures for 26 January. There are differences of up to -4 K at
70 about 30°S and 20°N, where the corrections for temperature gradients are important. Even so,
71 the comparisons with MERRA in Fig. S3 indicate that the V6 algorithm yields the more accurate
72 zonal mean temperatures from 30 to 50 hPa.

73

74 Figures S12 and S13 display V6 zonal average, ascending minus descending, orbital temperature
75 and ozone. Those differences are positive for both parameters, +1 K and +10 to 15%,
76 respectively, in the lower stratosphere at SH middle latitudes. Conversely, their differences are
77 both negative by about the same amounts at NH middle latitudes. The signs of the gradient
78 corrections depend on the orientation of the LIMS view path with respect to the isolines of

79 temperature in Fig. S9. The orientations of the along-path temperature gradients in the lower
80 stratosphere for ascending versus descending orbital views determines the signs of the
81 differences in both temperature and ozone—positive at SH and negative at NH middle latitudes.

82

83 A sequential estimation (SE) algorithm was used to obtain the V6 Level 3 zonal mean and zonal
84 wave coefficients from time series of the ascending and descending profile data points at a given
85 pressure and latitude. The SE fitting process attempts to follow the true amplitudes of zonal
86 waves, where the fitting is controlled by the estimated precisions of the input data. As an
87 example, Figure S14 shows the distribution of ozone at 46 hPa for 26 January for comparison
88 with that of temperature (Fig. S9). Figure S15 is the analogous ozone distribution at 68 hPa, and
89 where climatological ozone between $\pm 20^\circ$ varies from 0.68 to 0.55 ppmv. How well do their
90 zonal variations follow the Level 2 profile data? Table 1 gives ozone profile values at 30°S at
91 both 46 and 68 hPa for comparisons with Figs. S14 and S15. In general, the SE algorithm
92 follows the profile points, although the SE results tend not to follow the data extremes.

93

94 Examples of a rather poor fit of the SE coefficients to the profile data occur at 36°S and 46 hPa
95 for both temperature and ozone, which have rms differences of 3.5 K and 0.94 ppmv (39%),
96 respectively. The corresponding rms differences at 68 hPa are 3.8 K and 0.36 ppmv (55%).
97 Those rather poor fits also occur where the temperature gradient corrections are underestimated
98 and where the zonal averages of ascending minus descending orbital differences are as shown in
99 Figs. S12 and S13. In summary, the SE algorithm smooths the true zonal wave amplitudes in the
100 lower stratosphere. Larger amplitudes would give more pronounced zonal variations in SCO, but
101 then to a reduction of the wave amplitudes of TRCO, i.e., the negative TRCO values would
102 become less negative, and the positive values would become less positive.

103

104 Temperature biases are weaker and zonal wave variations are of smaller amplitude in the tropical
105 lower stratosphere in November 1978. As an example, Figure S16 shows V6 minus V5
106 temperatures for 8 November, when the largest differences occur between $\pm 20^\circ$ of latitude rather
107 than extending to the subtropics as on 26 January (Fig. S11). There is also a narrowing of the
108 latitude range of minimum temperatures in November (not shown) compared with that for
109 January (Fig. S10) that occurs because vertical transport in the tropics is weaker in November.
110 At any rate, climatological ozone values are relied upon at 68 and 100 hPa and between about
111 $\pm 20^\circ$ latitude to avoid residual cirrus effects in analyses of V6 SCO. Thus, it is posited that the
112 associated daily distributions of TRCO are representative of the spatial variations of tropical
113 tropospheric ozone during November 1978.

114

115 Figure S17 is the distribution of TRCO for 8 November but based on integrating SCO from 147
116 to 0.68 hPa. One can see that the elevated ozone at about 20°S , 0° longitude is nearly unchanged
117 from that in Figure 12 of the parent manuscript; it indicates ozone from lower in the troposphere.

118

119 **Figure credits:** Figures S10-S13 and S16 are screen shots of images viewable at
120 <https://lims.gats-inc.com/> and by clicking on Browse Images, Version 06, Day 026 or Day 312,
121 and then on Ltx (or latitude cross section).

122

123

124

125
126
127
128
129
130
131
132
133
134
135
136
137
138
139
140
141
142
143
144
145
146
147
148
149
150
151
152
153
154
155
156
157
158
159
160
161
162
163
164

Table 1

Level 2 Ozone Profile Data at ~30°S and at both 46 and 68 hPa on 26 January

Lon	46	68	A/D
Deg*	ppmv	ppmv	#
12	2.3	1.3	A
22	1.7	0.1	D
39	2.0	0.04	A
48	2.0	0.2	D
64	1.6	0.0	A
74	2.1	1.0	D
91	2.1	0.9	A
100	2.1	0.8	D
117	2.7	1.4	A
126	2.0	0.8	D
143	2.2	1.0	A
152	2.0	0.5	D
169	2.5	1.1	A
178	1.6	0.04	D

-171	1.9	0.03	A
-156	1.9	0.04	D
-130	1.4	0.02	D
-117	1.9	0.03	A
-104	2.1	1.0	D
-91	2.2	0.7	A
-77	2.2	0.4	D
-65	2.6	0.1	A
-52	1.4	0.04	D
-40	1.5	0.02	A
-29	1.8	0.03	D
-14	2.1	0.2	A

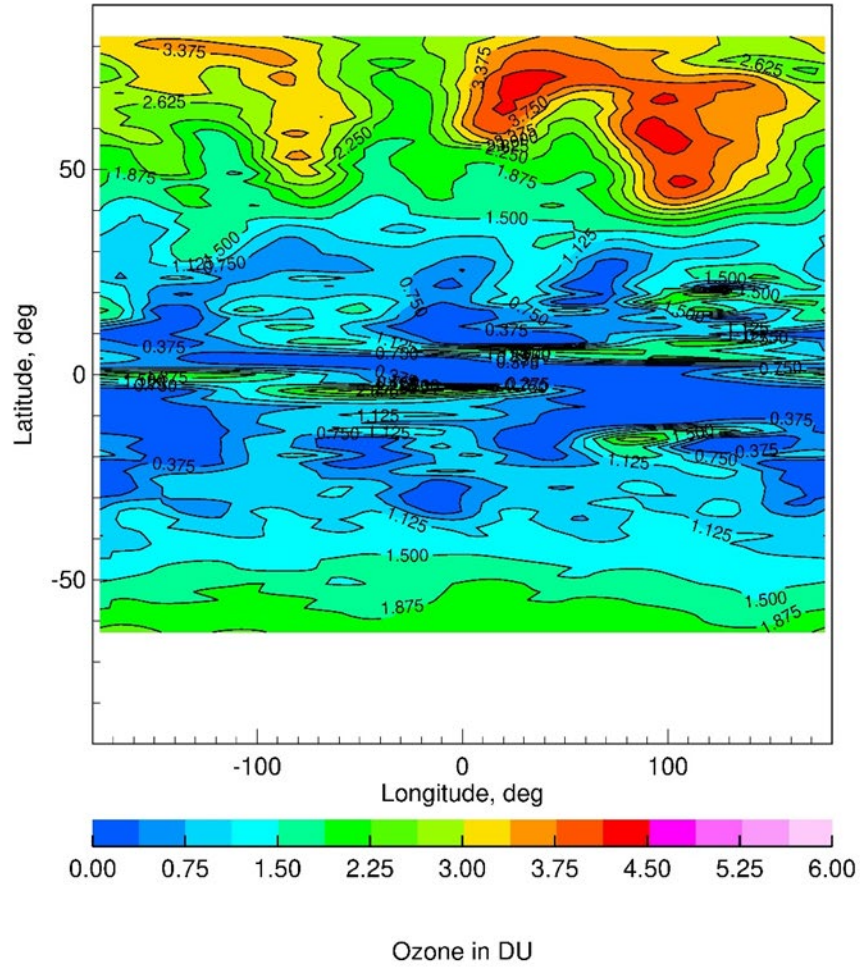
#A (or Asc) and D (Desc) orbits.

*pos is °E, neg is °W; the line --- partitions them.

There is no profile data near 30S on the Asc orbit between -156° and -130°.

165 **Figures**

166



167

168 Figure S1—Cylindrical map projection of V6 ozone at 68 hPa on 15 March 1979. There are
169 unexpected longitudinal structures in tropical ozone at this pressure level.

170

171

172

173

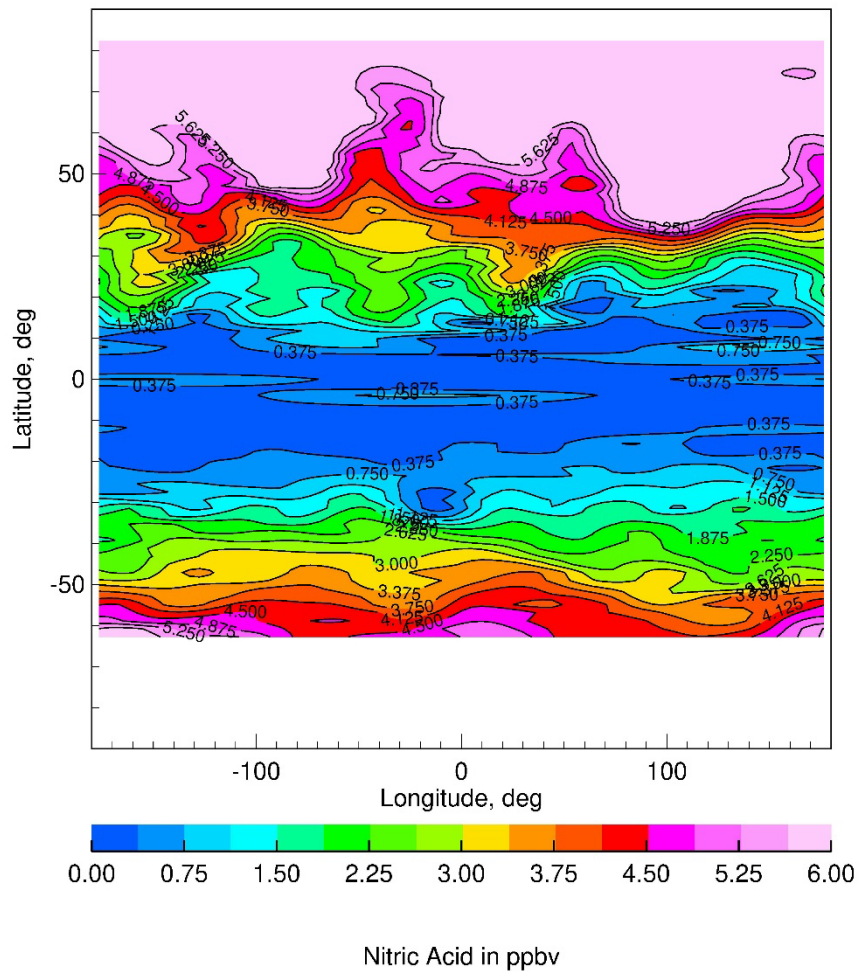
174

175

176

177

178



179

180 Figure S2—As in Fig. S1, but for V6 nitric acid at 68 hPa on 15 March 1979.

181

182

183

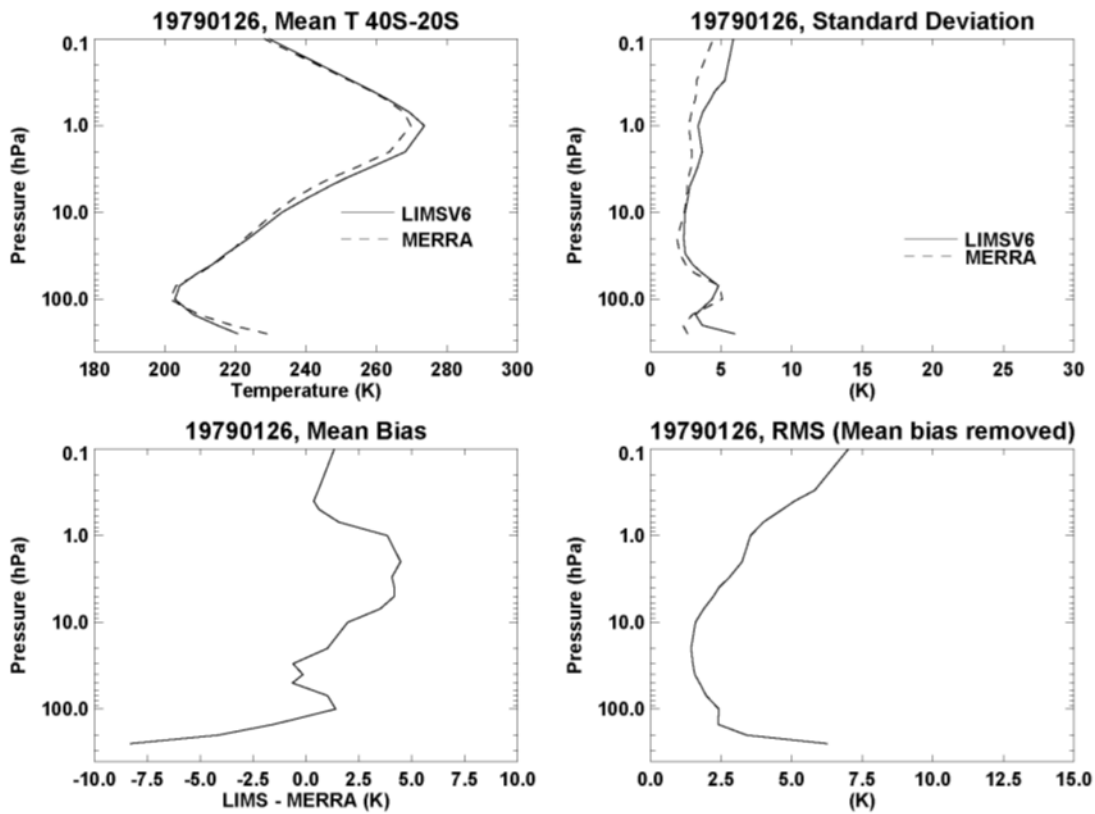
184

185

186

187

188
189

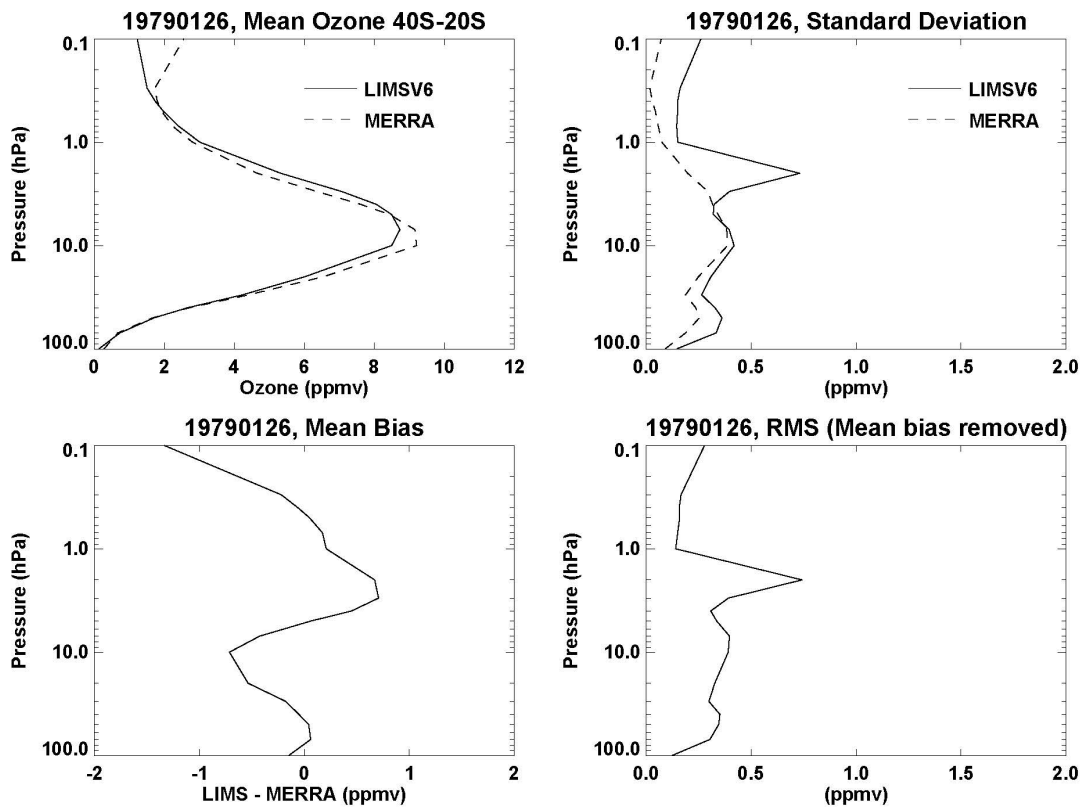


190
191
192
193
194
195
196
197
198
199
200
201

Figure S3—(top left) Temperature profiles from LIMS V6 versus MERRA for 40°S to 20°S. (bottom left) Mean bias, V6 minus MERRA, for 26 January 1979. (top right) standard deviation about the zonal mean, and (bottom right) RMS deviation with mean bias removed.

202

203



204

205 Figure S4—As in Fig. S3, but for ozone from 40°S to 20°S.

206

207

208

209

210

211

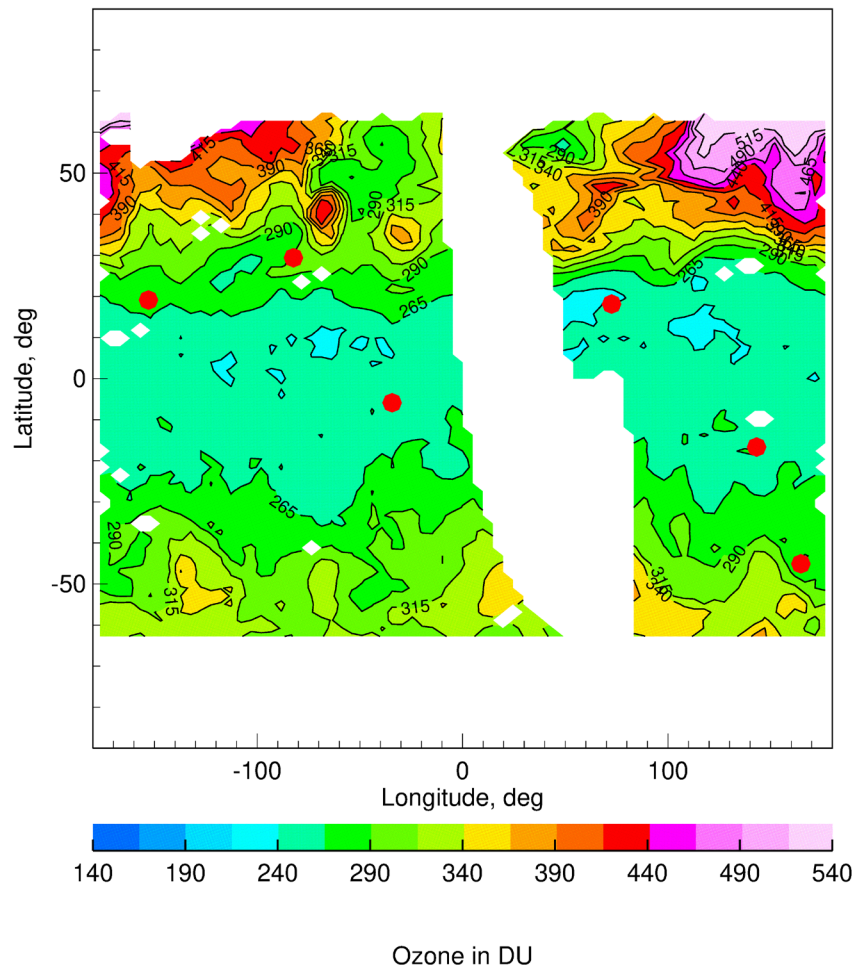
212

213

214

215

216



217

218 Figure S5—Distribution of TOMS ozone on 26 January 1979. White areas are where TOMS
219 made no measurements this day.

220

221

222

223

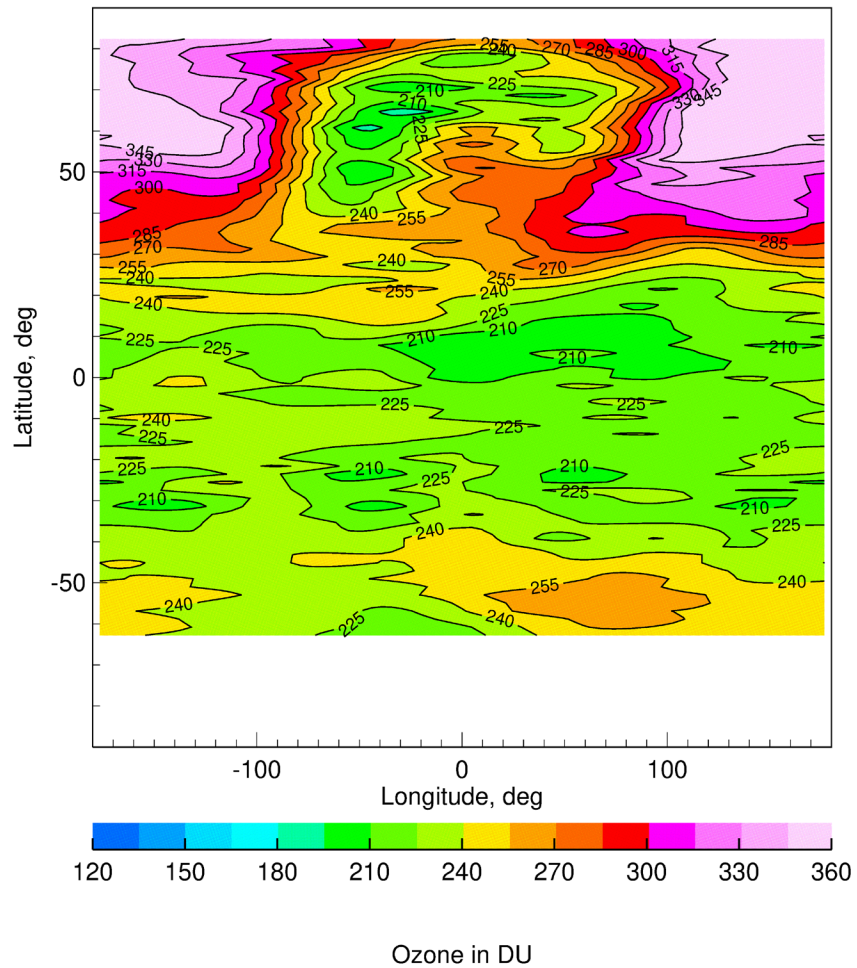
224

225

226

227

228



229

230 Figure S6—Distribution of SCO from 100 to 0.68 hPa on 26 January 1979.

231

232

233

234

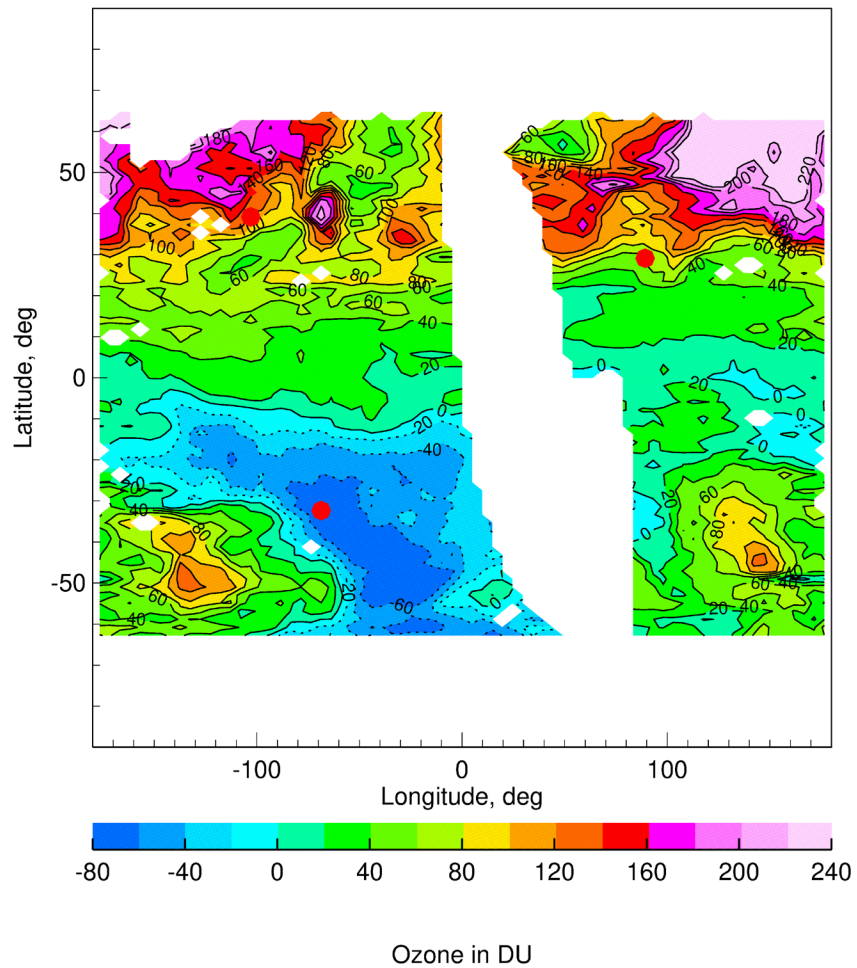
235

236

237

238

239



240

241 Figure S7—Distribution of TRCO values for 26 January 1979. The ozone scale is from -80 to
242 240 DU to accommodate negative values. Contour interval is 20 DU. Red dot at 33°S, 70°W is
243 location of Santiago, Chile.

244

245

246

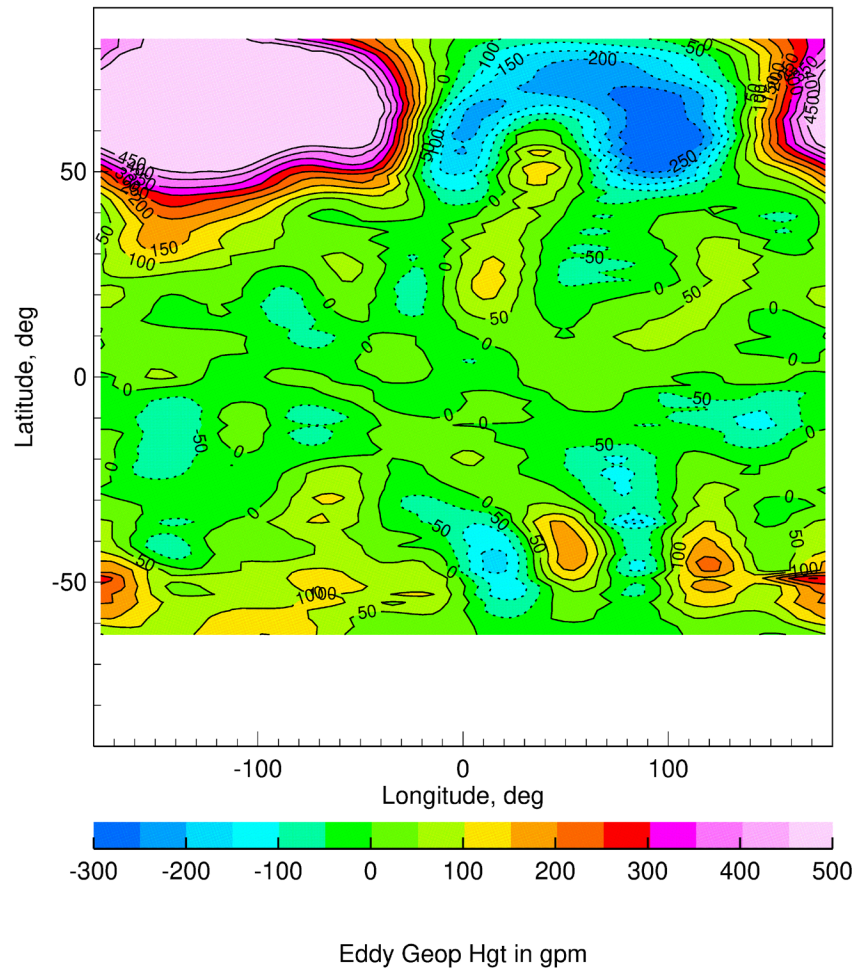
247

248

249

250

251



252

253 Figure S8—Contours of zonal eddy geopotential height on 26 January at 100 hPa.

254

255

256

257

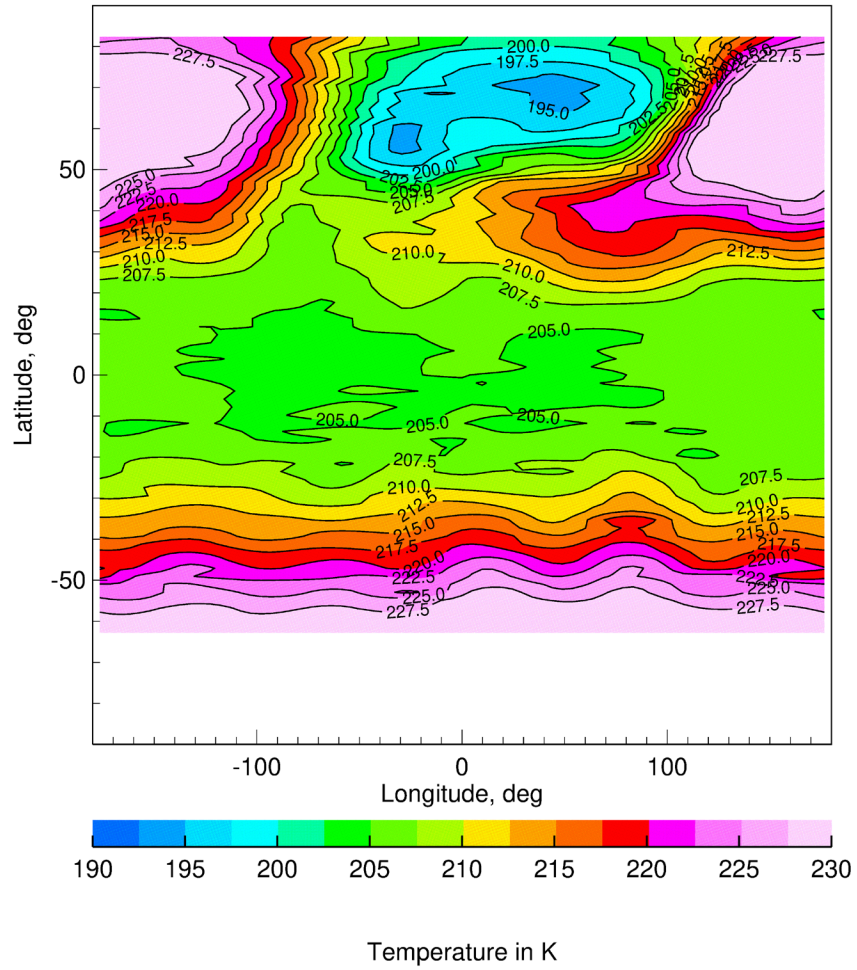
258

259

260

261

262



263

264 Figure S9—Distribution of V6 temperature on the 46 hPa surface for 26 January 1979. Contour
265 interval is 2.5 K.

266

267

268

269

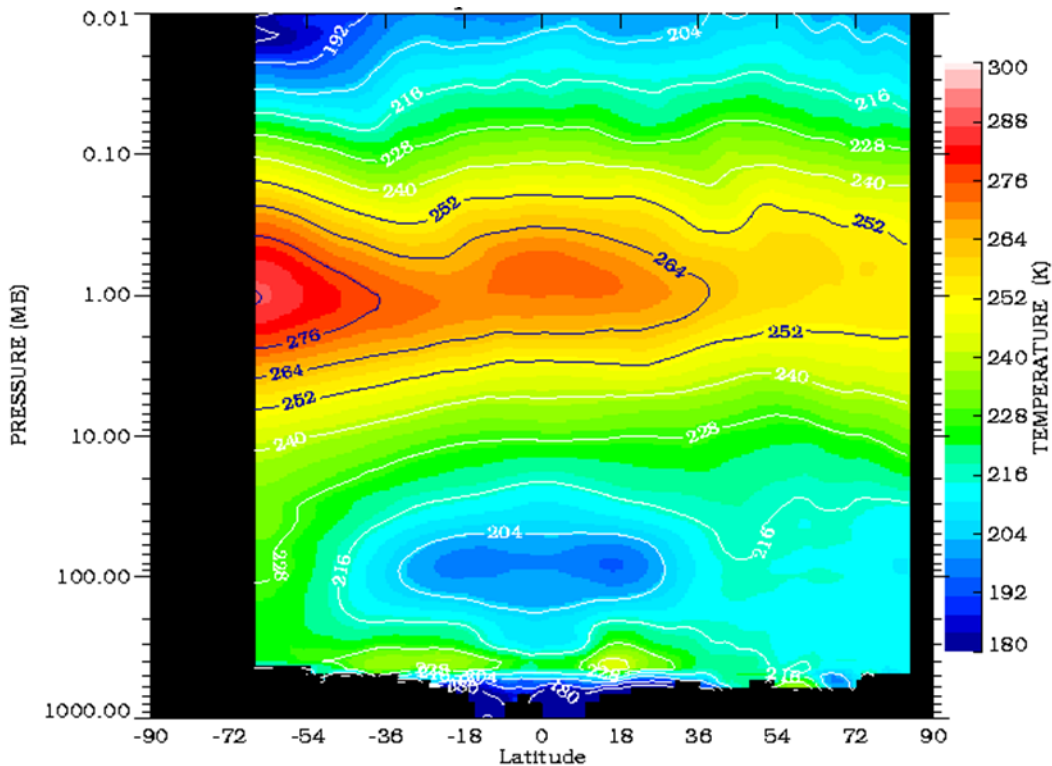
270

271

272

273

274



**TEMPERATURE Asc + Des Pressure vs Latitude
26-JAN to 27-JAN-1979**

275

276 Figure S10—V6 zonal mean temperature distribution on 26 January 1979. The terms, Asc plus
277 Des, refer to profile data taken in the alternate viewing directions of the LIMS ascending and
278 descending orbital segments.

279

280

281

282

283

284

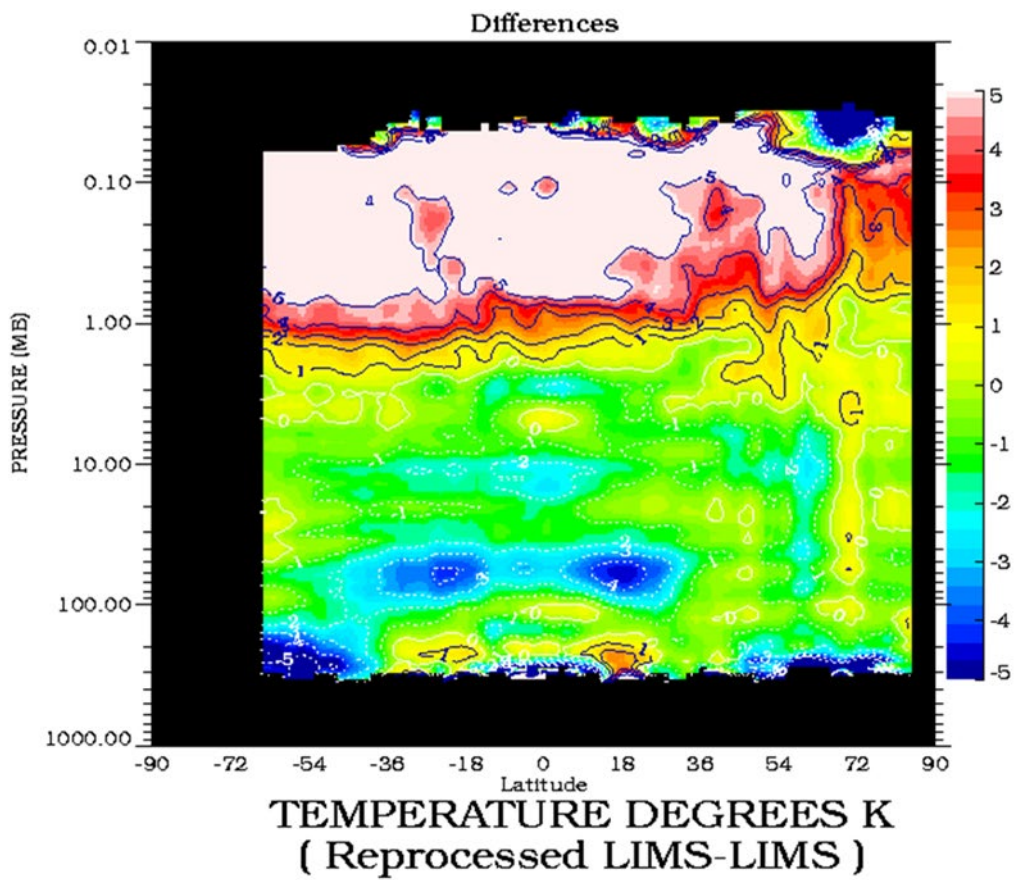
285

286

287

288

289



290

291 Figure S11—V6-V5 zonal average, temperature differences for 26 January 1979. The term
292 ‘Reprocessed LIMS’ refers to V6 and the term ‘LIMS’ to V5 in the label on the abscissa.

293

294

295

296

297

298

299

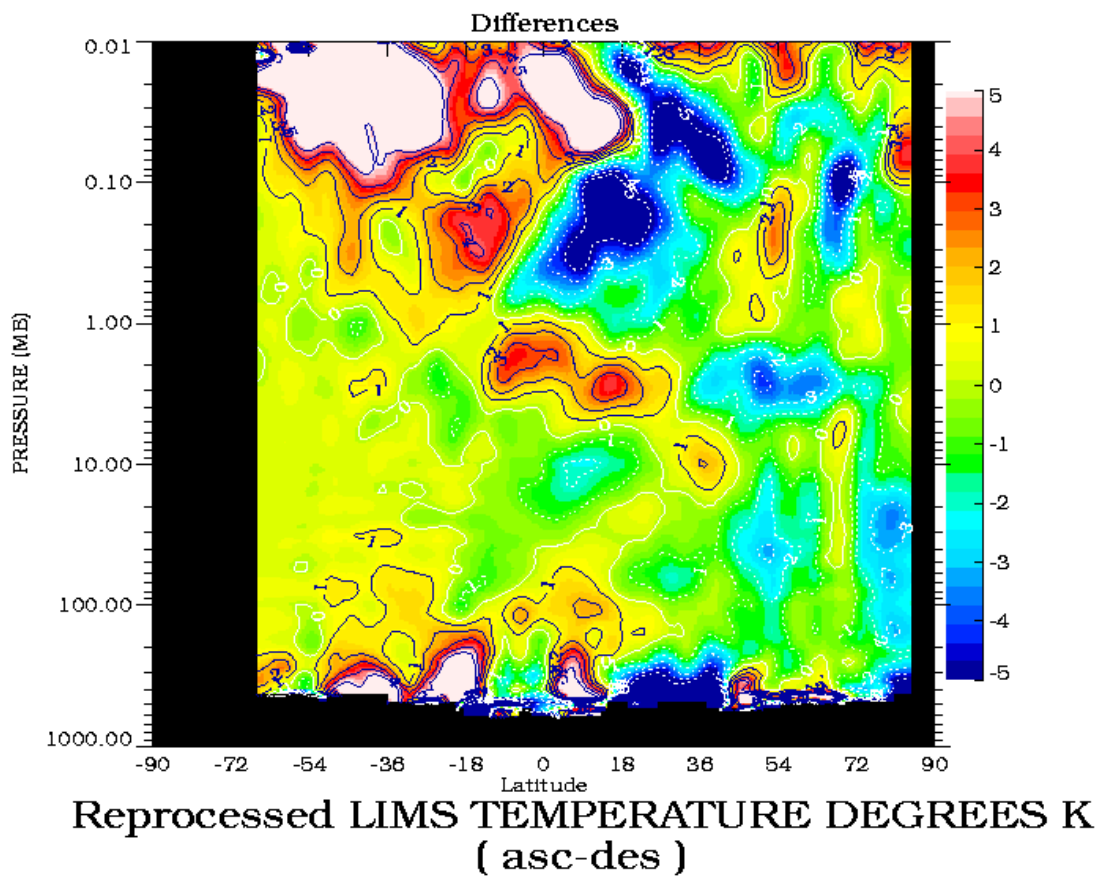
300

301

302

303

304



305

306 Figure S12—Zonal average of the ascending minus descending orbital temperature differences
307 (in K) from the V6 or ‘Reprocessed’ LIMS profile data for 26 January.

308

309

310

311

312

313

314

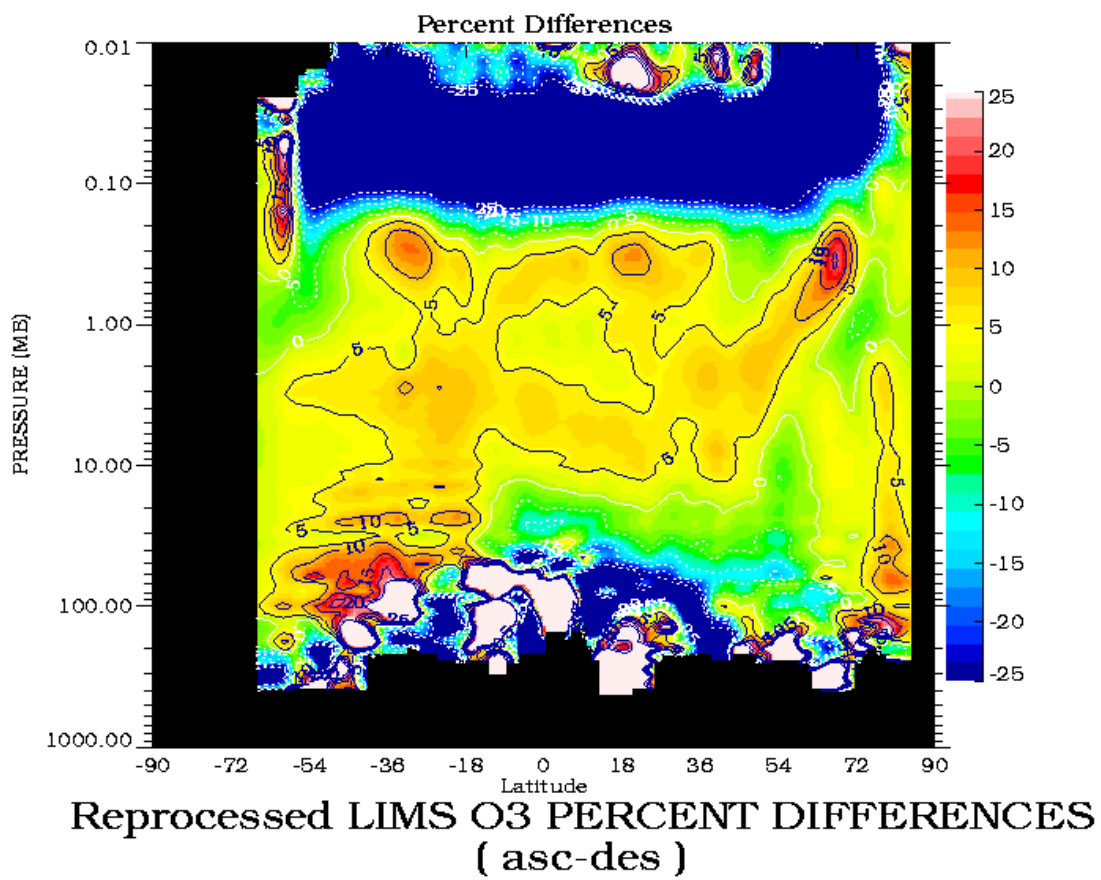
315

316

317

318

319



320

321 Figure S13—As in Fig. S12, but where the differences are for V6 ozone (in %).

322

323

324

325

326

327

328

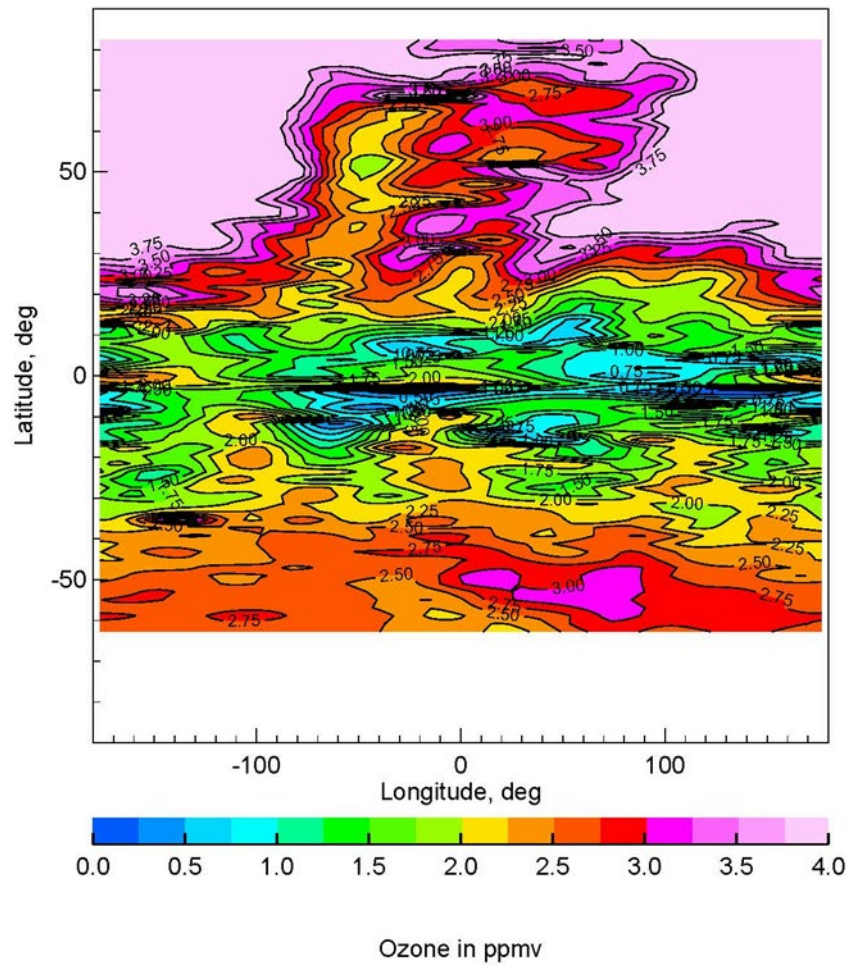
329

330

331

332

333



334

335 Figure S14—Distribution of V6 ozone on the 46 hPa surface for 26 January 1979.

336

337

338

339

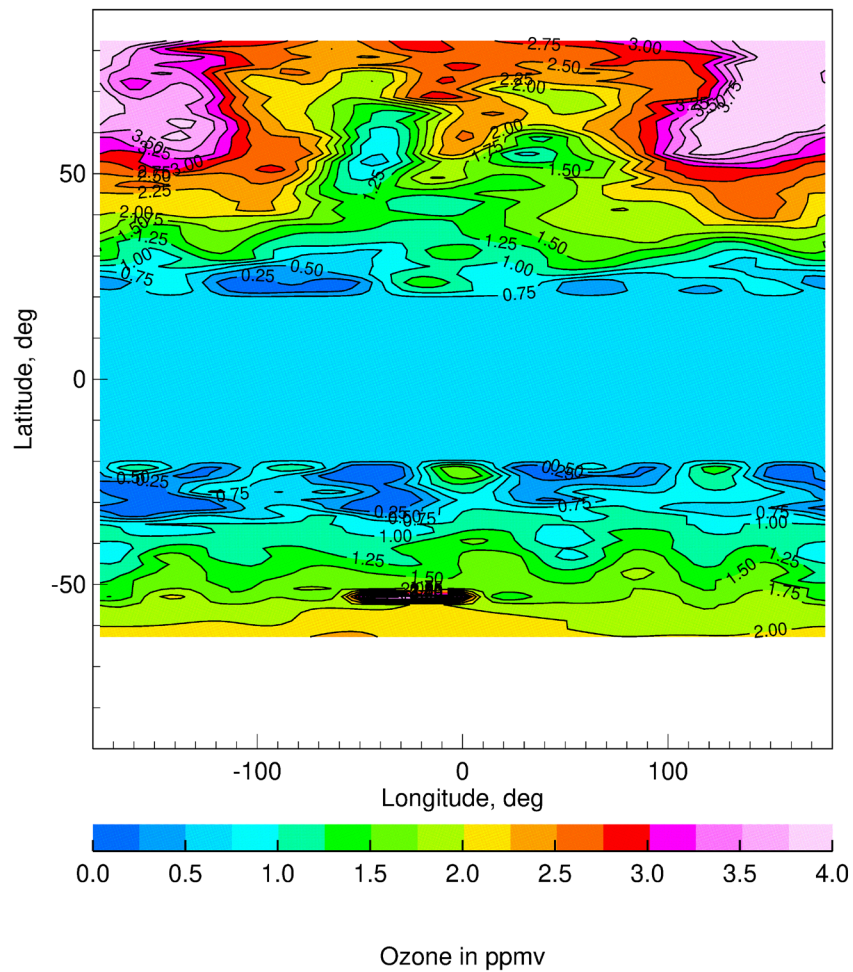
340

341

342

343

344



345

346 Figure S15—As in Fig. S14, but for ozone on the 68 hPa surface on 26 January 1979. LIMS
347 values have been replaced by zonal mean climatological values in the tropics.

348

349

350

351

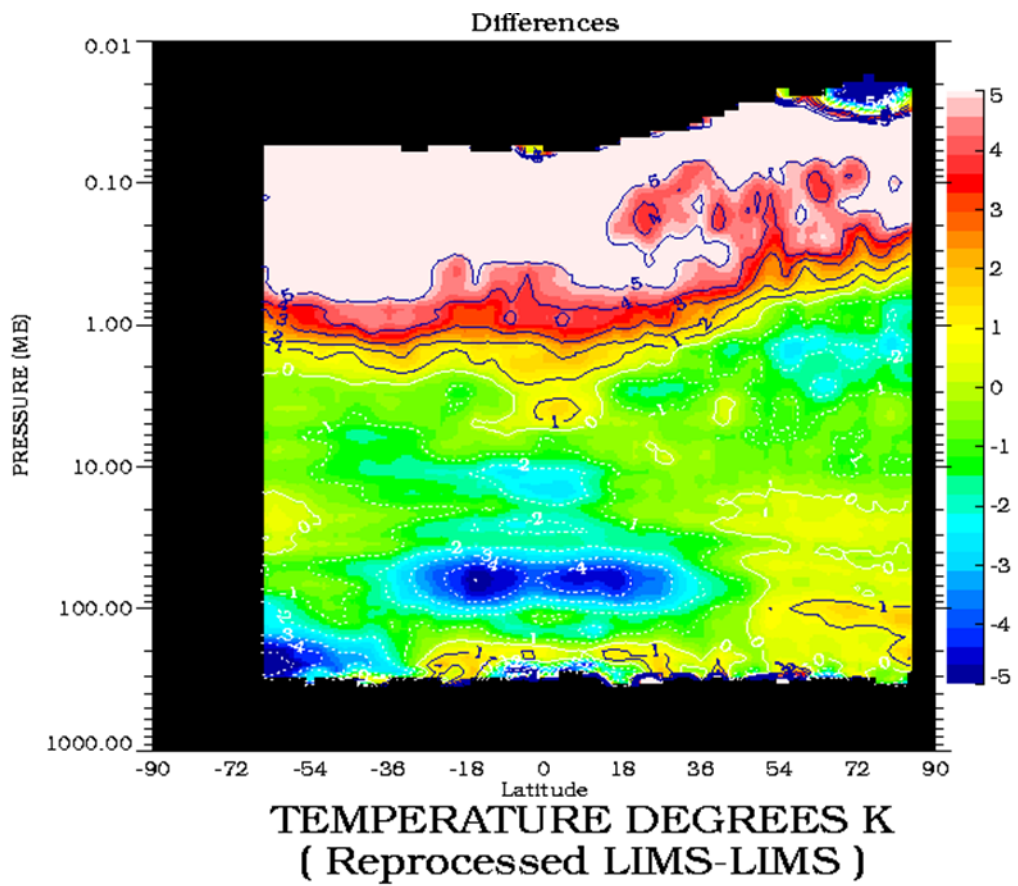
352

353

354

355

356



357

358 Figure S16—As in Fig. S11, but for 8 November 1978.

359

360

361

362

363

364

365

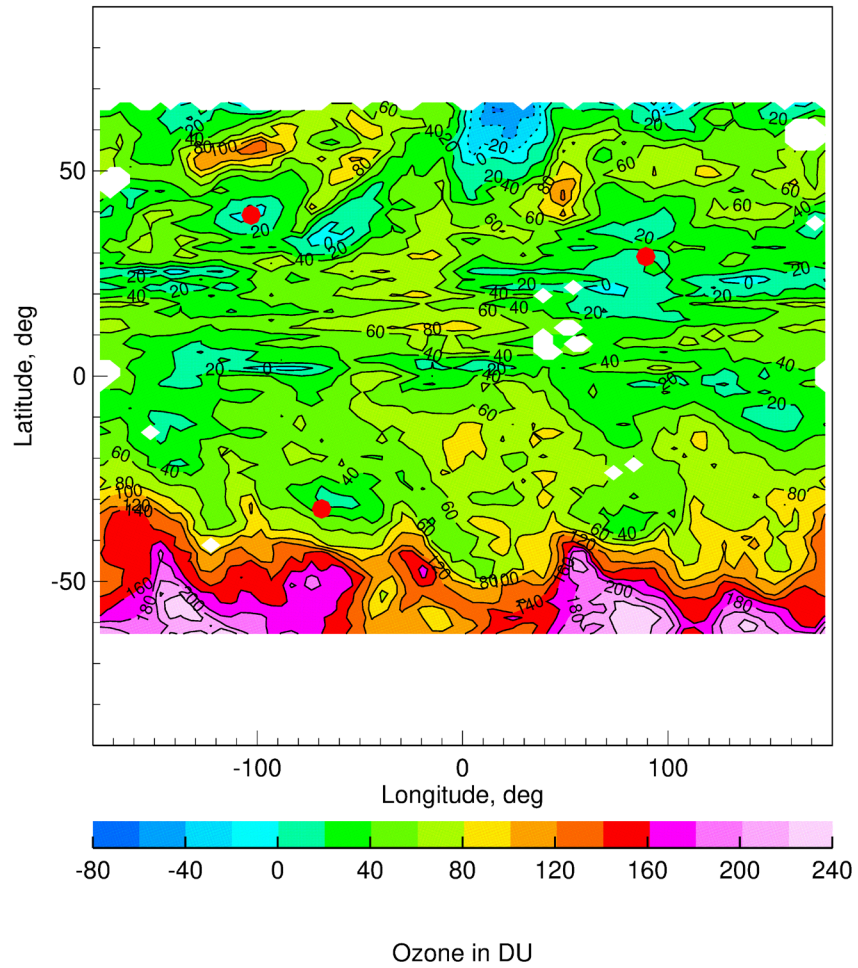
366

367

368

369

370



371

372 Figure S17—TRCO distribution for 8 November but based on integrating SCO from 147 to 0.68
373 hPa and for comparison with Figure 12 of the parent manuscript.

374